J Appl Electrochem (2013) 43:417–424
DOI 10.1007/s10800-013-0524-7

ORIGINAL PAPER

Electrochemical investigation of O_2-exposed Pd electrodes supported on YSZ

C. Jiménez-Borja · S. Souentie · J. González-Cobos · F. Dorado · J. L. Valverde

Received: 25 July 2012 / Accepted: 9 January 2013 / Published online: 18 January 2013

Abstract Cyclic voltammetry and steady state polarization measurements were performed for the electrochemical characterization of the O_2(g), Pd/YSZ system. The effect of oxygen partial pressure was investigated in the temperature range of 350–400 °C and it was found that under polarization phase transformations can take place. Application of negative potential values, lower than a threshold value of −0.6 V, can result in the decomposition of PdO, while the reduced species can be re-oxidized during a linear anodic potential scan. The results suggested that during the first minutes of cathodic polarization, the PdO reduc -tion reaction dominated versus the oxygen reduction reaction, while it becomes more significant as the oxygen concentration in the gas phase increased within the range 0–6 kPa.

Keywords Palladium electrode · YSZ · Cyclic voltammetry · Pd redox · Pd/YSZ interface · Electrochemical promotion

1 Introduction

Solid electrolytes can find several practical applications, such as in solid oxide fuel cells [1], gas sensors [2], electrochemical cells [3], batteries [4], chemical cogeneration systems [5], and electrochemical promoted catalysts [6]. Because of the industrial importance of catalytic oxidations and hydrogenations, oxygen ion and proton conductors are the most widely used solid electrolytes [7]. The most popular oxygen ion conductor is the 6–10 mol.% Y_2O_3-stabilized ZrO_2 (yttria-stabilized zirconia, YSZ). Its O^{2-} conductivity is based on the oxygen ion vacancies created in the lattice of the zirconia (tetravalent metal oxide) when it is doped with yttria (trivalent metal oxide). YSZ is an ionic conductor in the temperature range between 280 and 1200 °C. Owing to its chemical stability and mechanical strength [6–8], much attention has been focused on the electrochemical reactions that occur at the gas/electrode/solid oxide interfaces [9].

Palladium-based catalysts are considered as one of the most effective catalytic systems for oxidizing hydrocarbons, CO, or ethanol [10–13]. Palladium is extensively used as the active component in several industrial catalytic formulations of environmental technologies, as the destruction of harmful chemicals in gaseous emissions due to its excellent performance in the combustion of hydrocarbons and halocarbons, the thermal stability, and the low volatility of Pd particles [14]. Pd is mainly used in catalytic applications for the aftertreatment of emissions from stationary sources and especially in the field of catalytic total oxidation of hydrocarbons [15]. Thus, Pd is a promising catalyst for applications involving oxidation reactions including automotive catalytic converters and catalytic combustion of methane in advanced gas turbines where ultralow NO_x emissions are desired [16].

In this sense, it has been reported that the catalytic activity of Pd catalyst electrodes deposited on YSZ can be significantly enhanced under electrochemical promotion conditions [6] for CO_2 hydrogenation [17], ethylene

C. Jiménez-Borja (✉) · J. González-Cobos · F. Dorado · J. L. Valverde
Department of Chemical Engineering (UCLM), Avda. Camilo José Cela 12, Ciudad Real 13071, Spain
e-mail: Carmen.JBorja@uclm.es

S. Souentie
Department of Chemical Engineering, University of Patras, Caratheodory St1, Patras 26504, Greece

oxidation [18–20], methane oxidation [20–24], and reduction of NO by CO [25].

It is well known that the interaction between adsorbed O species and Pd is very complicated [26]. Moreover, the Pd–PdO transformation is rather important for oxidizing reactions since the dependence of the catalytic activity on the palladium state is quite complex [10]. It has been also demonstrated that the kind of the support can clearly affect the phase transformation as well as stabilize the catalytic active phase [27]. Therefore, the Pd/YSZ interface and Pd–PdO transformations are worth of deeper investigation.

Until now, only few works have been carried out on the electrochemical characterization of Pd catalyst electrodes deposited on YSZ. It has been verified that under polarization conditions, Pd–PdO consecutive phase transitions can take place [28–31]. Badwal and de Bruin [28] and Kaneko et al. [29] have investigated the Pd/YSZ interface as a function of temperature and oxygen partial pressure by AC impedance spectroscopy. They reported that the bulk and electrode resistances were abruptly changed at the decomposition temperature and pressure of PdO [28, 29]. Athanasiou et al. [30] and Kalimeri et al. [31] studied the electrode kinetics on the O_2, Pd/YSZ system by steady state polarization measurements. It was reported that the rate-determining step (rds) of the charge transfer reaction depended on the oxidation state of palladium [31]. Moreover, the interaction between oxygen and Pd is not limited to the formation of stoichiometric PdO, since substoichiometric compounds can be also formed [30]. Furthermore, Katsaounis [32] has investigated palladium electrodes deposited on YSZ via temperature-programed-desorption (TPD) of oxygen. He found that gaseous oxygen adsorption on palladium gave two adsorbed atomic oxygen species and the initial surface coverage of oxygen from the gas phase plays a very important role on the magnitude of the effect of polarization.

In this work, electrochemical characterization of the Pd/YSZ interface was carried out by cyclic voltammetry and steady state current–potential measurements. The effect of oxygen partial pressure within the range 0–6 kPa was investigated, in the temperature from 350 to 400 °C. It was found that phase transformations can occur upon varying the electrode's overpotential. Prolonged cathodic polarization can cause the decomposition of PdO, while the reduced species can be reoxidized during a linear anodic potential scan. Similar work has been done by Jaccoud et al. [33] and Fóti et al. [34] on the O_2 (g), Pt/YSZ system and by Souentie et al. [35] on the O_2 (g), Ni/YSZ system. In these studies, Pt–O species [33, 34] or NiO [35] were electrochemically formed by the O^{2-} species supplied from the electrolyte support upon anodic polarization.

2 Experimental

A Pd/YSZ/Au electrochemical cell was used in this study. YSZ pellet (8 mol.% Y_2O_3-stabilized ZrO_2, YSZ), of 19-mm diameter and 1-mm thickness (Henson Ceramics Limited) was used as the solid electrolyte. Inert gold counter and reference electrodes were deposited on one side of the solid electrolyte pellet by application of thin coatings of gold organometallic paste (Gwent Electronic Materials C1991025D2) followed by calcination at 850 °C for 2 h. A porous palladium catalytic film serving as the working electrode was deposited on the other side of the YSZ by impregnation technique. Working and counter electrodes were symmetrically placed to insure a symmetric current and potential distribution in the cell during electrochemical investigations, as discussed elsewhere [6].

Palladium catalyst-working electrode was prepared by successive steps of deposition and thermal decomposition of a palladium precursor solution. An aqueous solution of 0.1 M $[Pd(NH_3)_4](NO_3)_2$ (Sigma-Aldrich) was used as the precursor. Initially, 20 μl of the precursor were applied on the YSZ pellet, using a plastic circular mask to obtain 1.65-cm^2 geometric surface area. Then, evaporation of the solvent took place at 100 °C for 10 min, followed by drying of the sample at 120 °C overnight and then calcination at 450 °C for 2 h with a 5 °C min^{-1} temperature ramp. Several successive steps of deposition, drying, and heating were repeated in order to obtain a final metal loading of 0.85 mg Pd. The active area of the catalyst electrode film was determined by the electrochemical technique developed by Ladas et al. [36] and it was found to be 64 cm^2.

The experiments were carried out in an atmospheric pressure single chamber quartz reactor with a volume of 30 cm^3, as described in detail elsewhere [6, 24]. Before the experiments, the sample was pre-treated for stabilization under 20 % O_2, 100 cm^3 min^{-1} (STP) total volumetric gas flow rate at 300 °C for 2 h [22].

Praxair certified standards of O_2 (99.99 %) and He (99.999 %) were used. The total gas flow rate was controlled by a set of calibrated mass flowmeters (Brooks 5850 E and 5850 S) and was kept stable at 200 cm^3 min^{-1} (STP) in all the experiments. The temperature of the catalyst was measured with a K-type thermocouple (Thermocoax) placed inside a quartz tube in the proximity of the catalyst-working electrode. The reactor was placed in a furnace (JH HEE.CC4) equipped with a heating control system (Conatec 4801).

Electrochemical investigation of the palladium catalyst electrode was performed using a scanning potentiostat Voltalab PGZ 301 (Radiometer Analytical). For the determination of the ohmic drop, AC impedance spectra were recorded both under open circuit conditions and under polarization in the frequency range 10^5–0.01 Hz with an AC

amplitude of 20 mV superimposed to the catalyst overpotential. The measurements and data acquisition were carried out by the software Voltamaster 4.

In the figures, the presented potential difference between the working and the reference electrode, U_{WR}, is free of the ohmic component, unless stated differently, and also corrected with respect to the reference electrode exposed to O_2 partial pressure of 6 kPa. In the present experimental setup, the reference electrode was always exposed to the actual partial pressure of oxygen, P_{O_2}. Therefore, the mentioned necessary correction in U_{WR} was made according to the Nernst equation:

$$U_{WR}(6\ \text{kPa}) = U_{WR}(P_{O_2}) - RT/4F\ln(P_{O_2}/6\ \text{kPa}) \quad (1)$$

3 Results and discussion

3.1 Voltammetric investigation

Figure 1 shows the effect of temperature on the cyclic voltammograms of the Pd/YSZ system under oxygen atmosphere of 6 kPa with vertex potential values, U_{WR}, between −0.8 V and +1.0 V (IR-uncorrected values) and scan rate of 30 mV/s. The given voltammograms correspond to the 10th scan. It is shown that increasing the temperature, the general shape of the voltammograms remains almost the same. The main feature observed is the presence of an anodic peak, which becomes larger at higher temperatures. Moreover, significant current evolution is observed when the potential U_{WR} is lower than −0.4 V or higher than +0.8 V. The current evolving during anodic polarization ($U_{WR} > 0.5$ V) can be attributed to the oxygen evolution reaction (Eq. 2) that occurs at the working electrode tpb.

$$O^{2-}(YSZ) \rightarrow \tfrac{1}{2}\,O_2(g) + 2e^- \quad (2)$$

On the other hand, the observed current evolution under cathodic polarization ($U_{WR} < -0.4$ V) can be related to the oxygen reduction reaction at the working electrode tpb and/or to the PdO reduction to Pd.

XRD diffraction patterns of a similar electrode revealed that palladium oxide phase was only present on the fresh film. After the electrochemical investigation, metallic Pd was also detected [37], which is in accordance with thermodynamic data of PdO [38, 39]. It is likely that under negative potential application, PdO is partially electrochemically reduced to metallic palladium and then it is reoxidized during the positive potential scan. Thus, the observed anodic peak possibly corresponds to the following anodic reaction step (Eq. 3):

$$O^{2-}(YSZ) + Pd \rightarrow PdO + 2e^- \quad (3)$$

The absence of the corresponding cathodic peak may reflect the onset of a rapid electrochemical reduction process under the mentioned conditions (T, P_{O_2}), which are near thermodynamic PdO decomposition conditions.

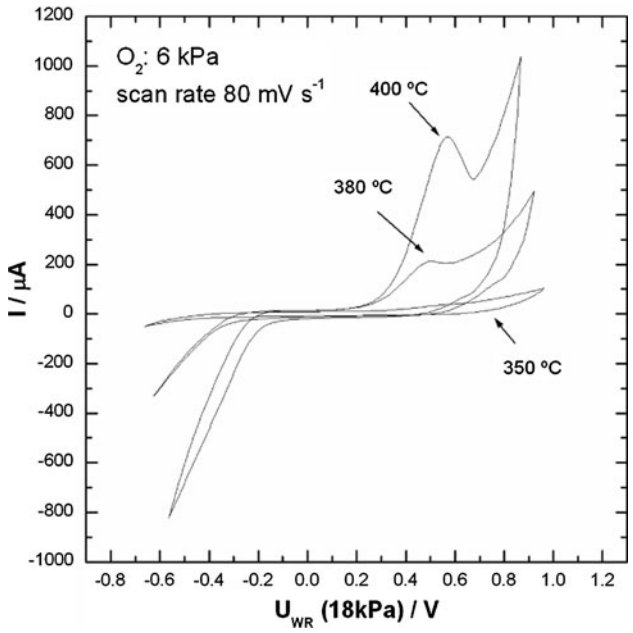

Fig. 1 Effect of temperature on the cyclic voltammogram of the Pd/YSZ system (10th cycle). $P_{O_2} = 6$ kPa and scan rate = 20 mV/s

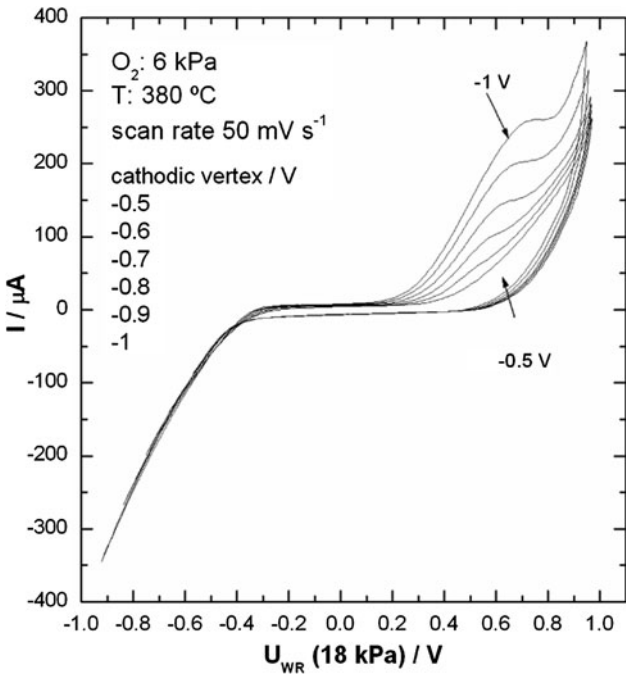

Fig. 2 Effect of cathodic vertex potential on the cyclic voltammogram of the Pd/YSZ system. $T = 380$ °C, $P_{O_2} = 6$ kPa and scan rate = 50 mV/s

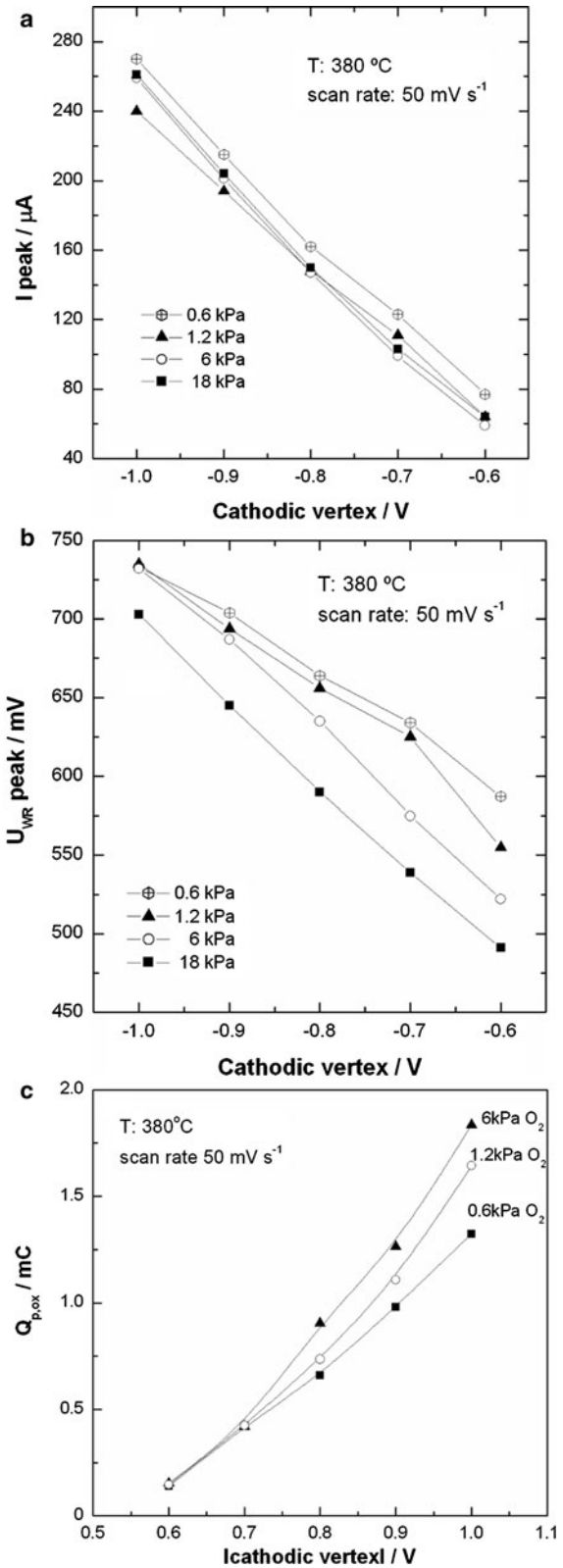

Fig. 3 Effect of cathodic vertex on the peak current, I_{peak} (**a**), on the peak potential, $U_{WR,peak}$ (**b**), and on the charge involved in the anodic peak, $Q_{p,ox}$ for different P_{O_2} (**c**). $T = 380$ °C and scan rate = 50 mV/s

It could be also attributed to a possible overlapping of the potential region of the PdO reduction reaction with that of the oxygen reduction reaction. The latter are further supported by the experiment shown in Fig. 2. In this figure, the effect of the cathodic vertex potential from −0.5 V to −1.0 V (IR-uncorrected values) on the voltammograms is shown at 380 °C under 6 kPa O_2 and scan rate of 50 mV/s. It seems that there is a threshold cathodic potential approximately at ∼−0.6 V above which the anodic peak appears. Moreover, the anodic peak increases with the vertex potential, which indicates the formation of higher amount of Pd at lower negative potential values. This threshold potential value is near the anodic peak potential, which varies from 0.5 V to 0.7 V by increasing cathodic vertex potential at 380 °C.

The effect of the cathodic vertex on the anodic peak characteristics for various oxygen partial pressures (P_{O_2}) in the 0.6–6 kPa range is presented in Fig. 3a–c. One can see that by shifting the cathodic vertex potential to more negative values, the peak current, I_{peak}, significantly increases following a linear dependence on the cathodic vertex (Fig. 3a). Peak potential, U_p, is shifted to more positive values (Fig. 3b) in the whole examined P_{O_2} range. On the other hand, as shown in Fig. 3c, the area of the anodic peak, $Q_{p,ox}$, increases with cathodic vertex.

The effect of the scan rate, υ, on the voltammograms is shown in Fig. 4a, for the case of 6 kPa O_2 at 400 °C. An increase in the scan rate from 5 to 150 mV/s leads to a slight shift of the peak to higher potential values, and also to a significant increase in the peak current, which is summarized in Fig. 4b for different temperatures and in Fig. 4c for different oxygen partial pressures. In both cases, a linear dependence of I_p on $\upsilon^{1/2}$ is observed, denoting an irreversible one-step one-electron case [40]. The increase of I_{peak} with P_{O_2} is in agreement with that observed in Fig. 3c, where $Q_{p,ox}$ increased by P_{O_2} under constant cathodic vertex. This positive effect of P_{O_2} on I_{peak} and $Q_{p,ox}$ could be possibly due to the higher amount of PdO formed chemically by gaseous O_2 at the vicinity of the electrode–solid electrolyte–gas phase tpb, which is then reduced under negative potential application. As shown, a power-law dependence of the charge on P_{O_2} exists, almost independent of the scan rate, i.e.$Q \approx cP_{O2}^{n}$, where n equals ∼ 0.15 (Inset Fig. 4c).

Experiments where the potential was initially kept constant at a fixed negative value (IR-uncorrected value of $U_{WR} = -0.8$ V) for different holding times (t_H) in the range 1–150 s with afterward linear potential scan toward +1.1 V were performed under 10 mV s^{-1} scan rate. The effect of the holding time, t_H, on the anodic peak of the voltammograms at 380 °C and under 0.6 kPa O_2 is shown in Fig. 5. The voltammograms shown here correspond to

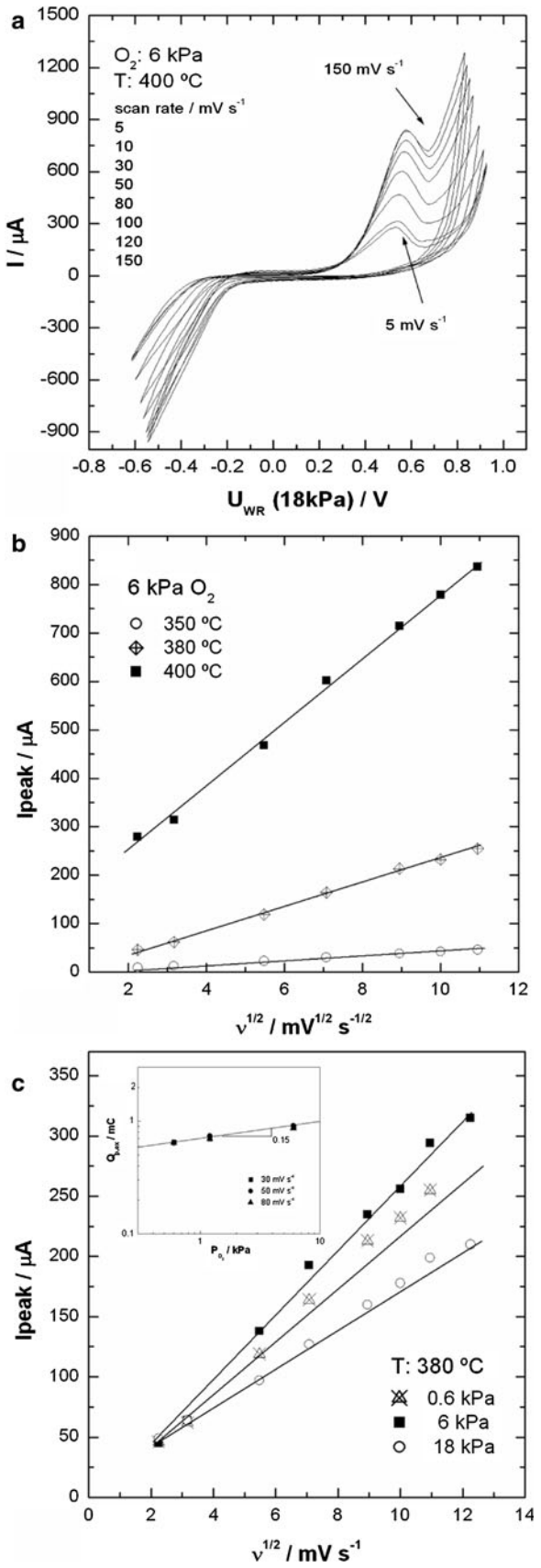

◀ **Fig. 4** **a** Effect of scan rate on the cyclic voltammograms of the Pd/YSZ system at $T = 400$ °C and $P_{O_2} = 6$ kPa (**a**). **b** Effect of scan rate on the peak current at three different temperatures: 350, 380, and 400 °C. $P_{O_2} = 6$ kPa. **c** Effect of scan rate on the peak current under three different P_{O_2}: 0.6, 1.2, and 6 kPa. $T = 380$ °C. *Inset* charge involved in the anodic peak

the first scan after the cathodic polarization. As shown, the longer the cathodic polarization time was, the larger the amount of PdO which was reduced is observed. Moreover, a shift of the peak toward more positive potential values is observed with t_H.

Figure 6a shows the effect of P_{O_2} on the charge involved in the anodic peak, $Q_{p,ox}$, within the P_{O_2} range of 0.6–6 kPa, under different holding times. The amount of Pd formed electrochemically and thus, the amount of the PdO formed via Eq. 3 during the anodic potential scan can be estimated by $Q_{p,ox}$. As shown, $Q_{p,ox}$ increases monotonically with holding time, t_H, while it becomes more pronounced under higher P_{O_2} (i.e. 6 kPa).

As mentioned before, under cathodic polarization, apart from the PdO reduction, the oxygen reduction reaction can also take place in parallel. The current efficiency for Pd formation, or equally PdO reduction, during cathodic polarization can be calculated by Eq. 4 [35]:

$$\varepsilon_{Pd} = Q_{p,ox}/Q_H \quad (4)$$

where $Q_{p,ox}$ is the charge involved in the anodic peak and Q_H is the given charge during the holding time t_H under cathodic polarization.

For a quantitative estimation of the contribution of each of the two parallel competitive electrochemical reactions, one can calculate the effective rate of PdO reduction, R_{eff}, on the basis of Eq. 5 [35]:

$$R_{eff} = I_{eff}/2F = I\varepsilon_{Pd}/2F \quad (5)$$

where I is the applied current during the cathodic polarization, I_{eff} is the effective current, used for Pd formation, and F is the Faraday constant.

Figures 6b, c show the effect of holding time under cathodic polarization on the current efficiency and effective rate of Pd formation, respectively, at different P_{O_2}. It is shown that initially ε_{Pd} is maximized, while an abrupt decrease is observed at longer holding times where ε_{Pd} reaches a plateau. Therefore, under cathodic polarization, initially the PdO reduction is the main electrochemical reaction, while at longer polarization times the oxygen reduction reaction dominates. Moreover, it seems that ε_{Pd} is strongly dependent on P_{O_2}. Under 0.6 kPa O_2, ε_{Pd} values close to 60 % were observed, while under 6 kPa O_2 the maximum ε_{Pd} is almost 100 % (Fig. 6b). This indicates that electrochemical reduction of PdO species takes place on both the gas-exposed electrode surface and the metal/electrolyte interface, in agreement with the observed

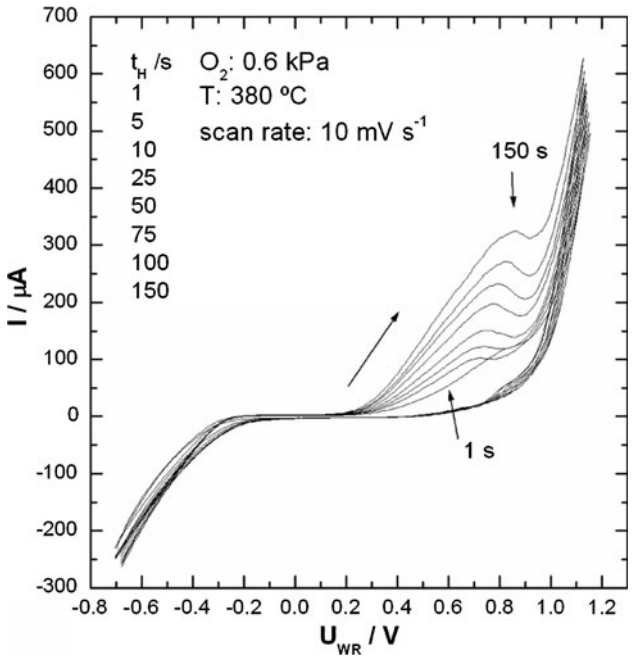

Fig. 5 Effect of holding time, t_H, at $U_{WR} = -0.8$ V on the cyclic voltammograms of the Pd/YSZ system (1st cycle). $T = 380$ °C, $P_{O_2} = 6$ kPa and scan rate = 10 mV/s

increase of $Q_{p,ox}$ with P_{O_2} for given cathodic vertex value (Fig. 3c).

Worth noting is the observed in Fig. 6c linear effect of $t_H^{-1/2}$ on the effective rate of PdO reduction reaction at the different P_{O_2}. Similar behavior has been reported for the electrochemical formation of NiO [35].

The effect of P_{O_2} on R_{eff} in the P_{O_2} range between 0.6 kPa and 6 kPa, is shown in the form of a log–log plot in Fig. 6d. The slope, as shown, is independent of the holding time and equal to ~ 0.37, indicating a behavior described by Eq. 6:

$$R_{eff} = k(T, U_{WR})\, P_{O2}^{0.37} \quad (6)$$

Experiments under prolonged cathodic polarization were performed only at 380 °C under application of −0.8 V. Thus, further experiments at different temperatures and negative applied potential values would be necessary to estimate the kinetic constant k, which only depends on temperature and applied potential. However, it appears that during cathodic polarization, the applied current is involved mainly in the O_2 reduction reaction, while under higher P_{O_2}, PdO reduction reaction dominates.

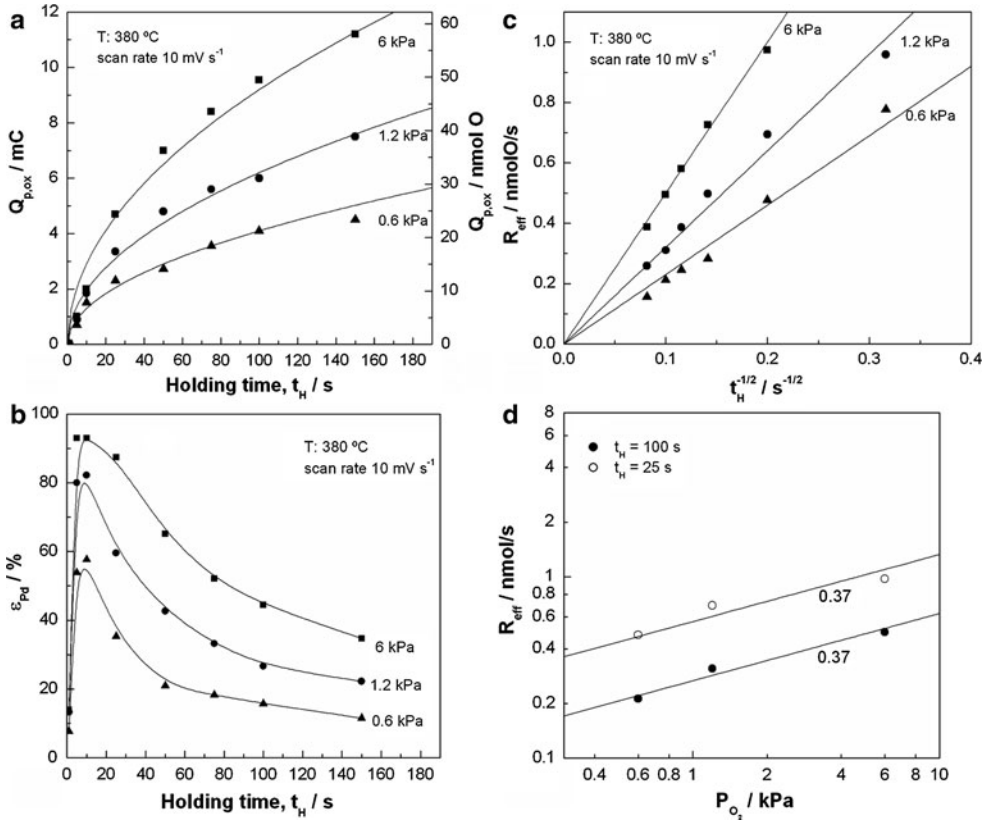

Fig. 6 Effect of holding time, t_H, for three different oxygen partial pressures: 0.6, 1.2 and 6 kPa on the charge involved in the anodic peak (**a**), on the current efficiency, εPd (**b**), and on the effective rate of PdO reduction (**c**), and the effect of P_{O_2} on the effective rate of PdO reduction for two different holding times: 25 and 100 s (**d**). $T = 380$ °C and scan rate = 10 mV/s

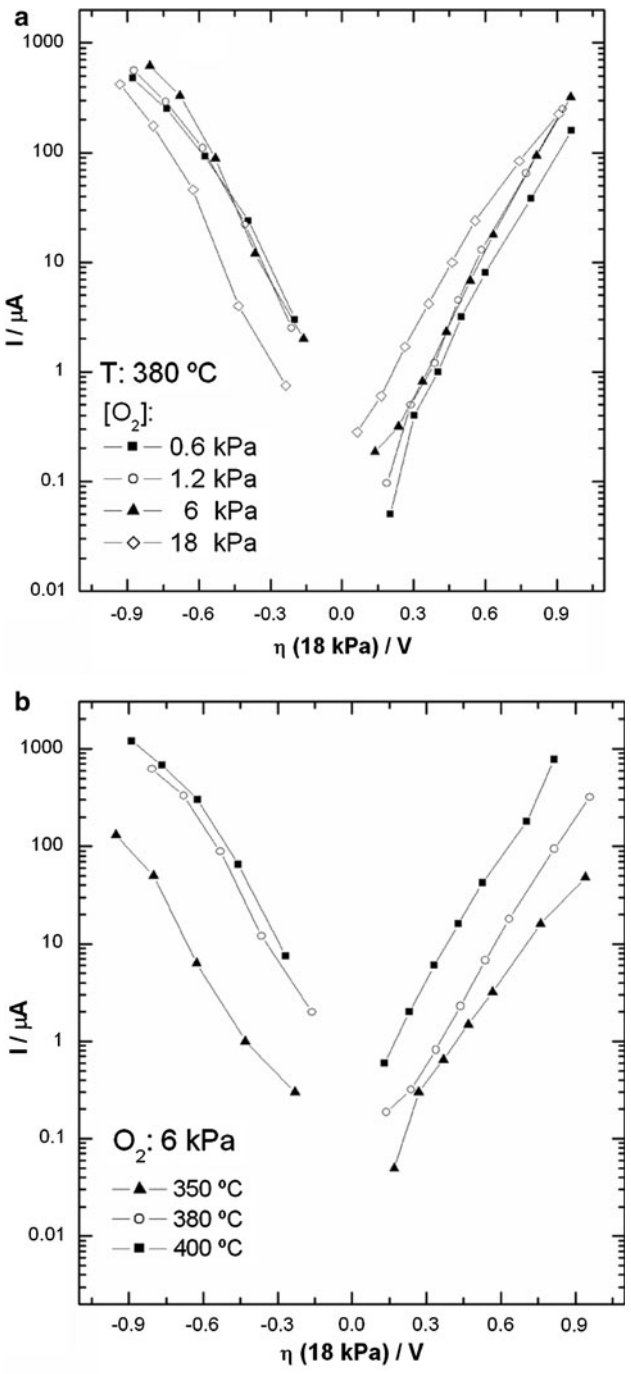

Fig. 7 Steady-state current-overpotential curves. Effect of P_{O_2} at 380 °C (**a**), and effect of temperature at $P_{O_2} = 6$ kPa (**b**)

3.2 Steady state polarization measurements

Steady state measurements were performed under potentiostatic mode and the obtained polarization curves are given in Fig. 7 in the form of Tafel plots. Overpotentials are IR-corrected values and also corrected with respect to the reference electrode exposed to O_2 partial pressure of 6 kPa. Figure 7a shows a comparison between the steady state current-overpotential curves under different P_{O_2} at 380 °C, while the effect of temperature under 6 kPa O_2 is presented in Fig. 7b. Limiting currents were not observed in the examined applied potential range.

As shown in Fig. 7a, higher currents were obtained in the case of negative potential application. This difference among the anodic and cathodic branches is in agreement with the cyclic voltammograms shown in the present study. Taking into account that under steady state conditions only the O_2 evolution reaction takes place upon positive polarization and only the O_2 reduction reaction occurs upon negative polarization; the observed lower currents upon positive polarization could be possibly due to inhibiting effects in the oxygen evolution reaction by the formation of PdO, which decreases the electronic conductivity. The latter is formed within the first few minutes of the anodic polarization, as shown in Fig. 6a–d, on both the metal-electrolyte interface and the electrode gas-exposed surface at the proximity of the gas/metal/electrolyte tpb.

Similar behavior in the polarization curve has been observed in the literature during electrochemical promotion of the deep methane oxidation on Pd/YSZ [24]. Badwal and de Bruin studied the electrode kinetics at the Pd/YSZ interface [28], where they reported a sharp change in the slope of the cathodic polarization curves, which was attributed to the low operating temperature, lower than the temperature for decomposition of PdO under the investigated value of P_{O_2}. Athanasiou et al. [30] also studied the electrode polarization at the O_2(g),Pd/YSZ interface under experimental conditions similar to the present study, but no significant difference in the current between positive and negative polarization was observed. This could be possibly due to the small applied cathodic overpotential values (~ -0.5 V), smaller than the threshold potential observed here (~ -0.6 V), which is required for the electrochemical reduction of the PdO, as shown in Fig. 2.

4 Conclusions

Electrochemical characterization of the O_2(g), Pd/YSZ system was carried out utilizing both cyclic voltammetry and steady state polarization measurements. It was found that the stability of the PdO/Pd system is a function of temperature, gas composition, and applied potential. Cathodic polarization, lower than -0.6 V, can lead to electrochemical reduction of PdO. Subsequent linear scanning of the potential toward the anodic region can cause electrochemical oxidation of the reduced species. These phase transformations which occur on the electrode are more pronounced at higher temperatures and depend

strongly on the surrounding gas atmosphere. During cathodic polarization, it was found that initially the PdO reduction was the main electrochemical reaction, while at longer polarization times the oxygen reduction reaction dominates. Moreover, the efficiency of the former was found to depend positively on P_{O_2}.

Acknowledgments Financial support by Science and Innovation Ministry of Spain [Projects CTQ2007-62512/PPQ and CTQ 2010-16 179/PQ] is acknowledged.

References

1. Larminie J, Dicks A (2003) Fuel cell systems explained. Willey, England
2. Skubal LR, Vogt MC (2004) Proc SPIE Int Soc Optical Eng 5586:45
3. Granqvist CG (1997) In: Gellings GPJ, Bouwmeester HJM (eds) The CRC handbook of solid state electrochemistry. CRC Press, Boca Raton
4. Julien C (1994) Solid state batteries: materials design and optimization. Kluwer, Boston
5. Vayenas CG, Farr RD (1980) Science 208:593
6. Vayenas CG, Bebelis S, Pliangos C, Brosda S, Tsiplakides D (2001) Electrochemical activation of catalysis: promotion, electrochemical promotion and metal-support interactions. Kluwer, New York
7. Garagounis I, Kyriakou V, Anagnostou C, Bourganis V, Papachristou I, Stoukides M (2011) Ind Eng Chem Res 50:431
8. Jaccoud A, Fóti G, Wüthrich R, Jotterand H, Comninellis Ch (2007) Top Catal 44:409
9. Chao T, Walsh KJ, Fedkiw PS (1991) Solid State Ionics 47:277
10. Ciuparu D, Lyubovsky MR, Altman E, Pfefferle LD, Datye A (2002) Catal Rev 44:593
11. Cargnello M, Delgado Jaén JJ, Hernández Garrido JC, Bakhmutsky K, Montini T, Calvino Gámez JJ, Gorte RJ, Fornasiero P (2012) Science 337:713
12. Colussi S, Trovarelli A, Vesselli E, Baraldi A, Comelli G, Groppi G, Lorca J (2010) Appl Catal A 390:1
13. Chen YX, Lavacchi A, Chen SP, di Benedetto F, Bevilacqua M, Bianchini C, Fornasiero P, Innocenti M, Marelli M, Oberhauser W, Sun SG, Vizza F (2012) Angew Chem Int Ed Engl 51:8500
14. Centi G (2001) J Mol Catal A 173:287
15. McCarty JG, Gusman M, Lowe DM, Hildenbrand DL, Lau KN (1999) Catal Today 47:5
16. Gélin P, Primet M (2002) Appl Catal B 39:1
17. Bebelis S, Karasali H, Vayenas CG (2008) Solid State Ionics 179:1391
18. Yiokari K, Bebelis S (2000) J Appl Electrochem 30:1277
19. Pliangos C, Yentekakis IV, Papadakis VG, Vayenas CG, Verykios XE (1997) Appl Catal B 14:161
20. Frantzis AD, Bebelis S, Vayenas CG (2000) Solid State Ionics 136–137:863
21. Giannikos A, Frantzis AD, Pliangos C, Bebelis S, Vayenas CG (1998) Ionics 4:53
22. Roche V, Karoum R, Billard A, Revel R, Vernoux P (2008) J Appl Electrochem 38:1111
23. Jiménez-Borja C, Dorado F, De Lucas-Consuegra A, García-Vargas JM, Valverde JL (2009) Catal Today 146:326
24. Jiménez-Borja C, Brosda S, Matei F, Makri M, Delgado B, Sapountzi F, Ciuparu D, Dorado F, Valverde JL, Vayenas CG (2012) Appl Catal B 128:48
25. Marwood M, Vayenas CG (1997) J Catal 170:275
26. Hu CC, Wen TC (1996) Electrochim Acta 41:1505
27. Ciuparu D, Pfefferle L (2001) Appl Catal A 209:415
28. Badwal SPS, de Bruin HJ (1982) J Electrochem Soc 129:1921
29. Kaneko H, Nagai A, Taimatsu H (1989) Solid State Ionics 35:257
30. Athanassiou C, Karagiannakis G, Zisekas S, Stoukides M (2000) Solid State Ionis 136–137:873
31. Kalimeri K, Pekridis G, Vartzoka S, Athanassiou C, Marnellos G (2006) Solid State Ionics 177:979
32. Katsaounis A (2008) J Appl Electrochem 38:1097
33. Jaccoud A, Falgairette C, Fóti G, Comninellis Ch (2007) Electrochim Acta 52:7927
34. Fóti G, Jaccoud A, Falgairette C, Comninellis Ch (2009) J Electroceram 23:175
35. Souentie S, Falgairette C, Comninellis Ch (2010) J Electrochem Soc 157:49
36. Ladas S, Bebelis S, Vayenas CG (1991) Surf Sci 251:1062
37. Jiménez-Borja C, Brosda S, Makri M, Sapountzi F, Dorado F, Valverde JL, Vayenas CG (2012) Solid State Ionics 225:376
38. Warner JS (1967) J Electrochem Soc 114:68
39. Peuckert M (1985) J Phys Chem 89:2481
40. Jaccoud A, Fóti G, Comninellis Ch (2006) Electrochim Acta 51:1264